Short-range order and electron structure of amorphous SiN_xO_y

I. A. Brytov, V. A. Gritsenko,[1] and Yu. N. Romashchenko

"Burevestnik" Scientific-Industrial Combine, Leningrad

The methods of x-ray electron and x-ray emission spectroscopy were used to study the electron structure of amorphous silicon oxynitride (a-SiN_xO_y) of variable composition ranging from SiO_2 to Si_3N_4. The short-range order in a-SiN_xO_y was described by a model of a disordered randomly bound network.

We shall report a study carried out by x-ray electron and x-ray emission spectroscopy methods, used to determine the electron structure of amorphous silicon oxynitride (a-SiN_xO_y) of variable composition from SiO_2 to Si_3N_4. We shall describe the structure of a-SiN_xO_y by a model of a disordered randomly bound network in which an atom of Si has a tetrahedral environment, an atom of N has a trigonal environment, and an atom of O binds two tetrahedra. The valence band consists of three subbands. The symmetry of the wave functions responsible for the valence band is established. It is shown that there are nonbonding $2p$ and $2p$ orbitals of N and O near the top of the valence band.

Amorphous silicon dioxide (a-SiO_2) and nitride (a-Si_3N_4) are binary compounds with the structure that can be described by the model of an ideal tetrahedral network.[1] Experiments on the diffraction of x rays in a-SiO_2 and the pulsed scattering of neutrons in a-Si_3N_4 (Ref. 2) indicate that the O–Si–O and N–Si–N angles in SiO_2 and Si_3N_4, respectively, are close to the ideal angle of $\approx 109°$ in a tetrahedron. Disordering of a-SiO_2 is due to the scatter of the Si–O–Si angles which vary within the range 120–180° with a maximum of the distribution function at 144° (Ref. 1). An elementary structural unit of a-SiO_2 is an $SiO_{4/2}$ tetrahedron and an oxygen atom in SiO_2 forms a bridge between two tetrahedra. In a-Si_3N_4 each N atom is bound to three Si atoms in trigonal positions. The elementary structure unit is $SiN_{4/3}$.

In the crystalline state there is a ternary compound, silicon oxynitride Si_2N_2O, which has the orthorhombic crystal structure[3] with a unit cell containing 20 atoms (an $SiN_{3/3}O_{1/2}$) tetrahedron is an elementary structure unit). In the amorphous state the composition of this oxynitride can vary from SiO_2 to Si_3N_4 because the synthesis takes place under strongly nonequilibrium conditions. A topological disorder in a-SiN_xO_y is complemented by an order due to fluctuations of the local atomic composition.

Depending on the characteristic scale of composition inhomogeneities (in other words, for different forms of the statistics of bonds), two models of variable-composition compounds can be distinguished.[4] In the random mixture (RM) model representing a disordered macroscopic mixture there are only two kinds of tetrahedra: SiO_4 and SiN_4 in our case. According to this model, a-SiN_xO_y represents a macroscopic mixture of two phases: SiO_2 and Si_3N_4. A model of a disordered mixture at the atomic level, known as the random bonding (RB), postulates that a-SiN_xO_y is a network of tetrahedra of different configurations.

The RB representations have been developed to explain the structure of a-SiO_x ($0 < x < 2$) in Refs. 4 and 5, but the experiments indicate that the short-range order in a-SiO_x is not described by the RB model.[5,6]

The band calculations of Si_2N_2O were carried out in Ref. 7 from first principles without fitting to the experimental data because of the absence of such data. The purpose of the present investigation was to determine the electron structure and the energy band structure of a-SiN_xO_y in a wide range of atomic compositions and to compare the experimental data with the theory in order to test its validity.

SAMPLES AND EXPERIMENTAL METHOD

Amorphous silicon oxynitride films of ≈ 1000 Å thickness were synthesized from a mixture of SiH_4, NH_3, and O_2 at $T = 875$ °C and the substrate was a single crystal of Si (1, 1, 1). The technology of preparation and the properties of the samples were described in detail in Ref. 8.

In x-ray spectroscopy the electronic levels of an atom (counted away from the nucleus) are denoted as follows:

Type of state	$1s$	$2s$	$2p$	$3s$	$3p$	$3d$	$4s$	$4p$	$\ldots$
Designation	K	L_1	$L_{2,3}$	M_1	$M_{2,3}$	$M_{4,5}$	N_1	$N_{2,3}$	$\ldots$

The double index denotes a spin doublet splitting of the relevant level. An x-ray emission spectrum is formed as a result of an allowed (obeying dipole selection rules) transition of an electron from an outer level to a vacancy in an inner shell of an atom.

Two methods of generating x-ray emission spectra can be distinguished in accordance with the method used to form a vacancy: the primary method when a vacancy is formed as a result of bombardment of a sample with a beam of electrons and a secondary (fluorescence) method in which vacancies result from irradiation of a sample with x rays generated by the primary anode. The x-ray absorption spectrum represents the transfer of electrons from the inner levels of vacant states in the conduction band. The x-ray emission lines are denoted in accordance with the level at which a vacancy responsible for the radiative transition is formed, whereas the absorption lines are denoted in accordance with the level from which an electron is released.

A set of x-ray spectra of the valence bands (representing electron transitions from the valence band to some inner level) and of the absorption spectra of different series and for different atoms in a compound gives an idea of the energy positions of the singularities of the density of states $N(E)$.

The relationship between the intensity in the x-ray spectrum $I(E)$ and the electron density $N(E)$, as well as the transition probability $P(E)$, can be represented by the following product:

$$I(E) \infty N(E) P(E).$$

Strictly speaking, the complex dependence of $P(E)$ on the electron characteristics in a crystal is not suitable for a direct calculation of the $N(E)$ curve from the intensities of the x-ray bands. Characteristic features of the x-ray bands correspond to singularities of the $N(E)$ curve, which make it possible to estimate qualitatively the total density of states $N(E)$, whereas a comparison of x-ray spectra belonging to different series and different atoms in a compound allows us to study the influence of $P(E)$ on the profile of the spectral band. The absorption coefficient $\mu(E)$ near an absorption edge can be described by a similar product:

$$\mu(E) \infty N(E) P(E),$$

i.e., the singularities of the initial absorption band are associated with the density of vacant states and with the transition probability.

Determination of the absorption spectra in the 1–7 Å range by the traditional transmission method (an analysis is made of the x rays transmitted by an absorber) presents no experimental difficulties. Investigation of the absorption spectra in the ultrasoft x-ray range 10–500 Å (precisely where the lines of such elements as B, C, N, and O are located) is difficult because of the need to prepare thin (100–1000 Å) homogeneous absorber films. Therefore, in this range the information on vacant states is obtained from the spectra of the quantum efficiency (yield) of the x-ray photoeffect of the investigated substance. This method is based on the fact that irradiation of a substance with x rays from the bremsstrahlung spectrum results in the emission of photoelectrons and Auger electrons and at energies of the incident radiation close to the absorption edges the number of these electrons varies proportionally to the absorption coefficient, so that observed pattern repeats the absorption spectra.

In the present study we determined the $L_{2,3}$ x-ray emission spectra representing the energy distributions of the occupied states of the s and d symmetry in the valence band and the nitrogen and oxygen K_α x-ray emission spectra representing the energy distributions of the states of the p symmetry in the valence band (wavelength range 150–23 Å). These spectra were obtained by the primary method using an RSM-500 x-ray spectrometer-monochromator with a spherical diffraction grating. The investigated samples were bonded to a water-cooled copper anode which was under a voltage of $+3$ kV. The current of electrons which excited x rays was 0.8–10 mA. Vacuum in the x-ray tube was at least 5×10^{-6} Torr. The intensities of the $L_{2,3}$ lines of Si, and of the K_α lines of N and O at the maxima were 400, 150, and 100 counts/sec, respectively.

The K_β x-ray emission spectra reflecting the energy distribution of the states of the p symmetry in the valence band and the K_α lines ($2p$–$1s$ transition) of silicon (wavelength range 6–7 Å) were obtained by a fluorescence method employing in SARF-1 spectrometer with a bent quartz crystal

of the $[10\bar{1}0]$ orientation. Vacuum in the x-ray tube was $\approx 1 \times 10^{-6}$ Torr. The fluorescence spectra were excited by bremsstrahlung from the W anode subjected to a voltage $V_a = 9$ kV and the current was $I_a = 0.4$ A. The intensities at the line maxima were $\sim 10^4$ and 10^2 pulses/sec for the K_α and K_β spectra of Si, respectively.

Information on the vacant states was obtained by recording the spectra of the quantum efficiency of the x-ray photoeffect. The K quantum efficiency spectra of Si were excited by bremsstrahlung from a Ta anode. The intensity at the maximum was ~ 200 pulses/sec and the contrast was 3–4. The $L_{2,3}$ quantum efficiency spectra of Si and the corresponding K spectra of N were excited by bremsstrahlung from the W anode. The intensity at the maximum was ~ 2000 and 100 pulses/sec, respectively, and the contrast for both spectra was at least 2. The energy resolution depended on the investigated part of the spectrum (in electron volts): at least 0.5 for the K x-ray emission and quantum efficiency spectra of Si; 0.5 for the K x-ray emission and quantum efficiency spectra of N; 0.2 for the $L_{2,3}$ quantum efficiency spectrum of Si; 0.4 for the $L_{2,3}$ x-ray emission spectrum of Si; 0.4 for the K x-ray emission spectrum of O; 0.8 for the K quantum efficiency spectrum of O.

The method of x-ray electron spectroscopy, which has become one of the fundamental physical methods for investigation of the structure of matter, provides valuable information which supplements x-ray spectroscopy. We used the method of x-ray electron spectroscopy to determine the energy position and width of an inner level at which a transition terminates, which made it possible to estimate the contribution of the level width to the total width of a particular spectrum and also to combine on a single energy scale the x-ray spectra belonging to different series and different atoms forming a given compound.

The physical essence of the method of x-ray electron spectroscopy, based on the Einstein equation for the photoelectric effect, consists of determination of the kinetic energy of an inner or valence (outer) electron knocked out from the investigated substance by an x-ray photon of known energy $h\nu$, and of determination of the ionization energy (binding energy) which is a sensitive characteristic of the chemical binding of a compound.

We investigated the x-ray electron spectra employing an HP 5960-A spectrometer using monochromatic radiation of the $K_{\alpha_{1,2}}$ line of aluminum as the excitation. Energy calibration was carried out using the $1s$ line of carbon, the binding of energy of which is $E_b = 285.0$ eV. The composition of a-SiN$_x$O$_y$ was determined by normalization of the intensities of the $1s$ lines of oxygen, nitrogen, and the $2p$ line of silicon to the known photoionization cross sections. The refractive index ($\lambda = 6328$ Å) and the composition of the investigated samples are listed in Table I.

SHORT-RANGE ATOMIC ORDER IN a-SiN$_x$O$_y$

If the structure of a-SiN$_x$O$_y$ can be described by the RM model, the x-ray emission spectrum corresponding to the $2s$ levels of Si should consist of two signals representing SiO$_2$ and Si$_3$N$_4$, as found earlier for a-SiO$_x$ (Ref. 6). The

TABLE I. Composition, refractive index, and absolute energies of A (Si$L_{2,3}$), A'(OK_α), and A'(NK_α) x-ray emission peaks (electron volts).

Sample no.	x	y	n	A(Si$L_{2,3}$)	A'(OK_α)	A'(NK_α)
7004	0,5	1,3	1,56	95,0	526,3	394,0
7066	0,8	0,8	1,66	95,1	526,2	393,9
2038	0,9	0,6	1,72	95,2	526,1	393,8
7026	1,1	0,4	1,79	95,5	526,2	393,5
2010	1,2	0,2	1,87	96,1	526,2	393,9
7792	1,3	0,1	1,92	96,5	526,7	393,9

experimental evidence shows that there is only one peak and the energy at its maximum decreases monotonically on increase in the proportion of oxygen (Fig. 1). Similar data are reported in Ref. 9 for the $2p$ levels of Si and for the $1s$ levels of N and O (Fig. 2). The monotonic variation of the binding energy of atomic levels as a result of variation of the composition of a-SiN$_x$O$_y$ shows that the structure of the latter is described by the RB model. In accordance with the RB model, a-SiN$_x$O$_y$ represents a network of tetrahedra of the SiN$_\nu$O$_{4-\nu}$ type, where $\nu = 0, 1, 3$, and 4. The oxygen atoms in such a tetrahedron replace the nitrogen atoms at random. In the case of a random substitution and on condition that an atom of N is coordinated by three Si atoms and an atom of O by two such atoms, the probability $W(\nu, x, y)$ of finding a tetrahedron of the configuration ν in a-SiN$_x$O$_y$ of a given composition (x, y) is

$$W(\nu, x, y) = \left(\frac{3x}{3x+2y}\right)^\nu \left(\frac{2y}{3x+2y}\right)^{4-\nu} \frac{4!}{\nu!(4-\nu)!}. \quad (1)$$

Equation (1) postulates the absence of Si–Si and broken bonds. Figure 3 shows the dependence (1) as a function of the parameter $z = 3x/(3x + 2y)$ representing the composition of all possible configurations of the tetrahedra. The probability of discovering a tetrahedron with a large value of the index rises on increase in the nitrogen concentration. The x-ray emission spectrum of the $2s$ levels of Si is a superposition of the signals corresponding to five types of tetrahedra with different values of the index ν. Since an increase in the index ν reduces the binding energy of the $2s$ level of Si, the combined peak shifts toward lower energies. The energy of the
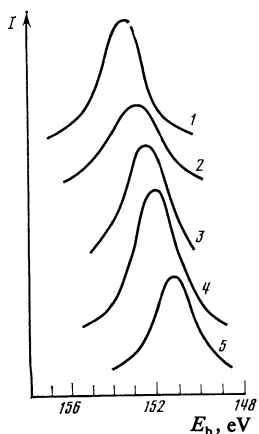
$K_{\alpha_{1,2}}$ line of Si in SiO$_2$ (Ref. 10) is practically the same as that of silicon in Si$_3$N$_4$ (Ref. 11), because the actual values are 1740.6 and 1740.5 eV, respectively. It therefore follows that the $2p$ and $1s$ levels of Si shift by an approximately the same amount when the environment of the silicon atom is altered.

Chemical shifts of the $1s$ levels of N and O (Fig. 2) indicate that a redistribution of the electron density in a-SiN$_x$O$_y$ occurs within at least two coordination spheres. In other words, the N and O atoms "sense" the environment of the Si atoms in which they are bound. In the opposite case the energies of the $1s$ levels of N and O are independent of the composition. An analysis of the composition of a-SiN$_x$O$_y$ (Fig. 4) shows that the following rule is obeyed[12]:

$$4 = 3x + 2y. \quad (2)$$

The equality (2) represents the familiar rule that the coordination number is $8 - m$, where m is the number of valence electrons of an atom. According to Eq. (2), an atom of Si forms four bonds with N or O, an atom of N bonds three tetrahedra, and an atom of O bonds two tetrahedra. Deviations from Eq. (2) can be explained by the presence of Si–H and N–H bonds in a-SiN$_x$O$_y$ in amounts representing a few atomic percent.[14]

ELECTRON STRUCTURE OF a-SiN$_{x \approx 1.1}$O$_{y \approx 0.4}$

The x-ray electron spectra of a-SiN$_x$O$_y$ are presented in Fig. 5. The density-of-states peaks with energies $\sim$30 and $\sim$25 eV in a-SiN$_x$O$_y$ correspond to the positions of the $2s$ levels of O and N. A comparison of the photoionization cross

FIG. 1. X-ray electron spectra of the $2s$ levels of Si in a-SiO$_2$ (1), in a-Si$_3$N$_4$ (5), and in variable-composition a-SiN$_x$O$_y$: 2) $x = 0.5, y = 1.3$; 3) $x = y = 0.8$; 4) $x = 1.2, y = 0.1$.
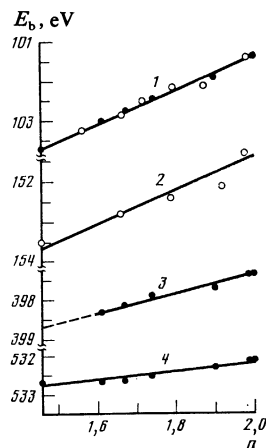

FIG. 2. Energies of $2p$ levels of Si (1), $2s$ levels of Si (2), $1s$ levels of N (3) and $1s$ levels of O (4) in a-Si$_3$N$_4$, a-SiO$_2$, and a-SiN$_x$O$_y$ plotted as a function of the refractive index of the wavelength $\lambda = 6328$ Å (O represents our data and ● represents the results from Ref. 10).
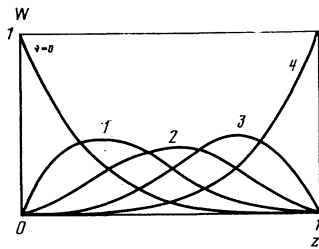
FIG. 3. Probability of detection of a tetrahedron of configuration v, in the RB model, plotted as a function of the parameter $z = 3x/(3x + 2y)$ representing the composition.

sections of the $3s$ and $3p$ levels of Ni, and of the $2p$ levels of N and O (Ref. 15) shows that the main contribution to the intensity corresponding to the upper parts of the valence band comes from the $3s$ orbitals of Si; the $L_{2,3}$ emission spectra of Si (representing electron transitions from the valence band to the $2p$ level of Si) reflect the distribution of the $3s$, d states of Si, whereas the K_β spectra of Si represent the density of the $3p$ states of Si, and the K_α spectra of N and O represent the densities of the $2p$ states of N and O, respectively. The same selection rules are satisfied by the experimental results on x-ray absorption. We investigated the quantum efficiency spectra which, as shown in Ref. 16, are similar to the absorption spectra.

Figure 6 shows x-ray emission and quantum efficiency spectra of a-SiN$_{1.1}$O$_{0.4}$ similar in composition to crystalline Si$_2$N$_2$O. The known values of the binding energies of the $2p$ levels of Si and the $1s$ levels of N and O (Fig. 2) are used to reduce all the spectra in Fig. 6 to the same origin which represents the electron energy in vacuum. The K_α x-ray emission spectrum of Si in crystalline Si$_2$N$_2$O is taken from Ref. 17. It is fitted to the other spectra allowing for the energy of the $K_{\alpha_{1,2}}$ line of Si.

The dipole selection rules for the x-ray transitions and the results of a calculation of the electron structure of crystalline Si$_2$N$_2$O (Refs. 7 and 18) can be used to identify various features in the x-ray spectra: the maxima denoted by C_1 and C_2 correspond to a group of molecular orbitals (MO) dominated by the contribution of the $2s$ atomic orbitals (AO) of oxygen and nitrogen, respectively, with the admixture of the $3s$ and $3p$ atomic orbitals of Si. The maxima B, B′, and A reflect the σ and π bonds due to the interaction of the $3s$, $3p_\sigma$, $3p_\pi$ AO of Si with the $2p_\sigma$ and $2p_\pi$ AO of N and O. The main maximum, denoted by A′, of the K_α bands of O and N represents the nonbonding MO consisting of the $2p_\pi$ AO of O and N.

FIG. 5. X-ray electron spectra of the valence band of a-SiO$_2$ (1), a-Si$_3$N$_4$ (4), and a-SiN$_x$O$_y$ (2 corresponds to SiN$_{0.49}$O$_{1.26}$ and 3 corresponds to SiN$_{1.26}$O$_{0.11}$). The energies are measured from the electron level in vacuum.

Our experiments do not allow us to identify the partial contribution of the $3d$ states of Si, but the results of calculations relating to Si$_2$N$_2$O (Ref. 7), α and β forms of Si$_3$N$_4$ (Ref.
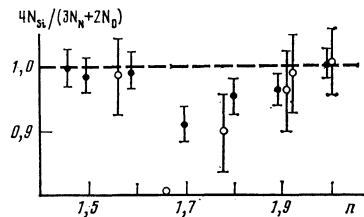

FIG. 4. Ratio of the number of bonds of silicon to the number of bonds of nitrogen and oxygen plotted as a function of the refractive index of a-SiN$_x$O$_y$ (O represents our results and ● represents data from Ref. 13).
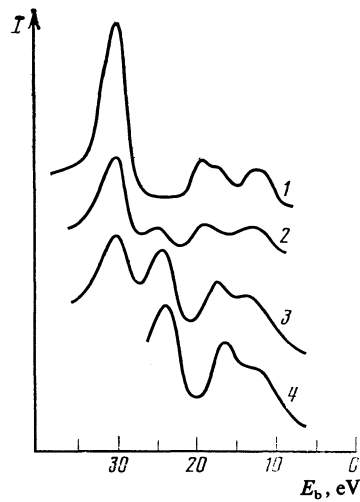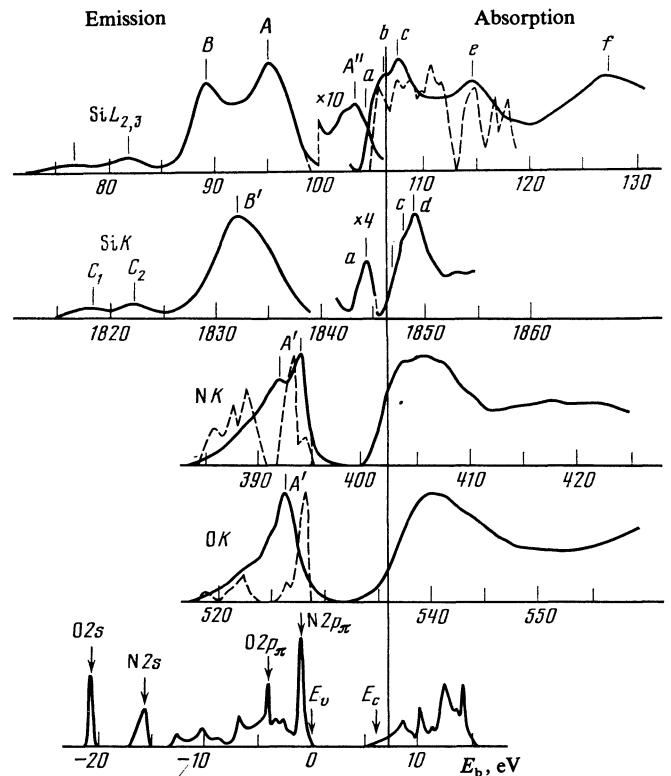
FIG. 6. X-ray emission and quantum efficiency spectra of Si, N, and O atoms in a-SiN$_{1.1}$O$_{0.4}$. The K emission spectrum of Si in Si$_2$N$_2$O is taken from Ref. 17. The total density of states in Si$_2$N$_2$O taken from Ref. 18 is plotted at the bottom of the figure. The spectra are reduced to the single energy scale. The origin corresponds to the electron energy in vacuum (vertical continuous line). The arrows identify the positions of the edges of the E_c and E_v bands deduced from the data on internal photoemission and absorption taken from Ref. 8. The dashed curves are the partial densities of states of the Si, N, and O atoms taken from Ref. 7.

19), and SiO_2 (Ref. 20) are evidence of a small contribution of the $3d$ orbitals of Si to the formation of the valence band. The model calculation of the electron structure of Si_2N_2O reported in Ref. 18 and the more accurate calculations of Ref. 7 (Fig. 6) demonstrate the existence near the top of the valence band of nonbonding $2p_\pi$ orbitals of N and O, which is in general agreement with the results of our experiments. However, in contrast to the experimental results, the $2p_\pi$ orbital of O is—according to Ref. 7—located above the $2p_\pi$ orbital of N. An energy gap between a subband formed from the $3s$ and $3p$ states of Si hybridized with the $2p$ states of O and N, and the subband formed from the nonbonding $2p_\pi$ orbitals of N and O (Fig. 6) does not correspond to the calculated x-ray spectra reported in Ref. 7. This discrepancy is, in our opinion, due to the following factors:

1) the finite width of the levels involved in the x-ray transitions and the instrumental broadening of the spectra;

2) the overlap of the MO groups as a result of deviation of the configuration of the tetrahedron and the nature of the linkage of the tetrahedra in a-$SiN_{1.1}O_{0.4}$ from the corresponding situation in an ideal crystal;

3) inaccuracies of the calculation method.

The $L_{2,3}$ x-ray emission spectrum of Si has a maximum A'' at ~ 103 eV, similar to that reported for a-Si_3N_4 (Ref. 9), and the relative intensity of this maximum is approximately one-twentieth of the maximum denoted by A. The nature of the additional maximum cannot be explained by the results of calculations of the electron structure of Si_2N_2O reported in Refs. 7 and 18. In our opinion, by analogy with a-Si_3N_4, this maximum represents the occupied states related genetically to the $3s$, d states of Si and split off to this part of the energy band. Interpretation of the absence of reliable calculations of the electron structure in the region of vacant states of nitrides of group III elements which would allow for the exciton effects and for the relaxation of the outer shells.

In accordance with the calculations of Refs. 7 and 18, the main contribution to the density of vacant states comes from the Si states and an allowance for the $3d$ orbitals of Si (in the α and β forms of Si_3N_4) increases the density of the vacant states near the bottom of the conduction band.[19] Bearing in mind also the dipole rules for the x-ray tansitions, we can propose the following identification of the main maxima in the quantum efficiency spectra: a maximum denoted by a in the K quantum efficiency spectrum of Si and a hump a in the $L_{2,3}$ spectrum of Si (which coincide on a unified energy scale) represent a level formed by the $3d$-AO^* state of Si hybridized with an admixture of the $2p$-AO^* states of N and O; the main contribution to a level denoted by b is made by the vacant $3s$-AO^* states of Si with the $2p$-AO^* admixture due to N; the levels denoted by c and d are formed mainly from the contribution of the vacant $3p$-AO^* states of Si and $2p$-AO^* states of N and O containing an admixture of $3d$-AO^* from Si; finally, the levels denoted by e and f consist of contributions of $3d$-AO^* from Si and $2p$-AO^* from N (here, AO^* are the vacant orbitals).

The experiments on the internal photoemission of electrons from Si and Al in a-$SiN_{1.1}O_{0.4}$, reported in Ref. 8, given an electron affinity $\varkappa = 1.6$ eV (defined as the separa-

tion from the bottom of the conduction band E_c to the electron level in vacuum). The optical width of the band gap of a-$SiN_{1.1}O_{0.4}$, determined by extrapolation of the $(\alpha\hbar\omega)^{1/2} - \hbar\omega$ dependence to zero absorption coefficient, amounts to $E_g = 5.7$ eV. This values is in satisfactory agreement with the "x-ray" width of the band gap $E_g = 6.1$ eV, equal to the energy gap between the top of the valence band (E_v) and the bottom of the conduction band (E_c). The position of E_v is determined from the $L_{2,3}$ x-ray emission spectra of Si and the K_α emission spectra of O and N by linear extrapolation of their short-wavelength edges to the point of intersection with the background. This method of determination of E_v and E_g gave earlier good results in the case of Al and Si oxides[11] and also in the case of Ref. 9. Theory predicts the value $E_g = 5.97$ eV for Si_2N_2O (Ref. 7).

INFLUENCE OF THE ATOMIC COMPOSITION ON THE DENSITY OF STATES IN VARIABLE-COMPOSITION a-SiN_xO_y

A series of investigations has been carried out on the influence of the atomic composition of a-SiO_x on the density of electron states.[21,22] A similar study has not yet been made in the case of a-SiN_xO_y. Figure 7 shows the $L_{2,3}$ x-ray emission and quantum efficiency spectra of Si and the corresponding K spectra of N and O. The spectra are combined on the same energy scale relative to the Fermi level of an electron spectrometer. Table I gives the absolute values of the energies at the maxima of the $L_{2,3}$ emission spectra of Si and of the K emission spectra of N and O.
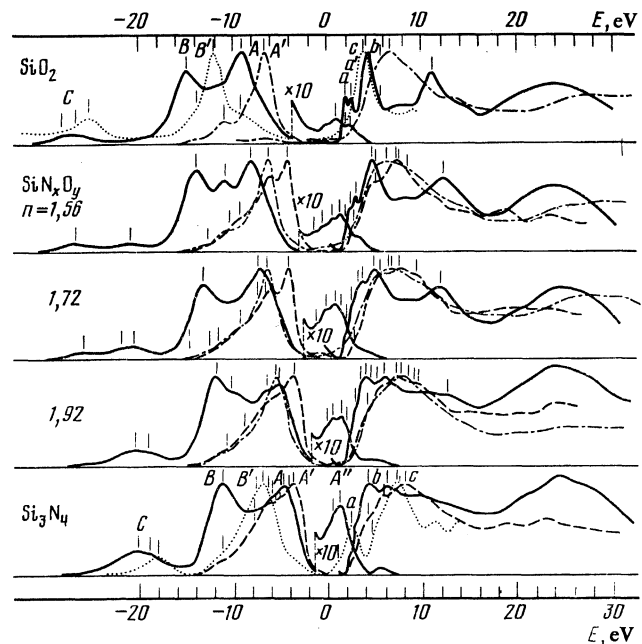

FIG. 7. X-ray emission and absorption spectra of variable-composition a-SiN_xO_y: the continuous curves represent the $L_{2,3}$ spectra of Si (lower scale), the dotted curves and the K spectra of Si, the dashed curves and the K spectra of N, and the chain curves are the K spectra of O. The K spectra of N and O obtained for each sample are fitted using the energies of the $1s$ levels of N and O; the zero energy point is taken to be the Fermi level of the electron spectrometer (corresponding to the $1s$ and $2p$ levels of Si and to the $1s$ levels of N and O); E is the relative energy of x-ray quanta due to the various transitions.

It follows from Fig. 7 that the relative positions of the partial density-of-states peaks of a-SiN$_x$O$_y$ are qualitatively the same for all compositions. The observed shifts to the energies of the maxima confirm the RB model. In the RM model the peak positions would have been constant for different compositions. The shifts of the density-of-states peaks manifested in the emission spectra are in qualitative agreement with the shifts of the LVV Auger spectra of Si in variable-composition a-SiN$_x$O$_y$ (Ref. 23).

Enrichment of a-SiN$_x$O$_y$ with oxygen is accompanied by an increase in the relative contribution of the $3s$, d states of Si to the upper part of the valence band (A' maximum in the $L_{2,3}$ spectrum of Si).

The $L_{2,3}$ x-ray emission spectrum of Si has a maximum A'' observed at ≈ 1 eV on the reduced energy scale (Fig. 7) and the relative intensity of this maximum is an order of magnitude less than the intensity of the A maximum in the $L_{2,3}$ spectrum of Si, and it decreases in the direction from a-SiN$_4$ to a-SiO$_2$. A hypothesis on the nature of this maximum has been put forward above in a discussion of a-SiN$_{1.1}$O$_{0.4}$. Agreement between the initial part of the absorption spectrum of the N and O atoms in SiN$_x$O$_y$ indicates hybridization of the vacant states of these atoms in the region of the conduction band.

The Si–N bond length is less than the sum of the covalent radii of Si and N, which is explained in Ref. 24 by postulating an interaction between the $3d_\pi$ states of Si and the $2p_\pi$ states of N in Si$_3$N$_4$. Similar ideas have been put forward for SiO$_2$ in Ref. 25. Our experimental results provide a clear evidence on this point.

Figure 8 shows the experimentally determined diagram of the levels in the investigated compounds. We can see that in the Si$_3$N$_4$, SiN$_x$O$_y$, SiO$_2$ series the value of $\varkappa$ decreases monotonically from 2 to 1 eV and E_g rises from 4.5 to 9 eV, in agreement with the optical absorption experiments[8]; the ionization energy of the $3s$ levels of Si (represented by the B maximum in the $L_{2,3}$ x-ray emission spectrum of Si) rises from 15.8 to 19.4 eV; the ionization energy of the $2p_\pi$ levels

of N and O varies to a lesser degree and increases approximately by about 0.8 eV the splitting between them amounting to 1.5 eV for $n = 1.92$ and then remain practically constant on increase in n (≈ 2 eV); the relative intensity of the a maximum in the K quantum efficiency spectrum of Si decreases, but for samples with $n < 1.79$ this maximum is hardly noticeable and the energy gap $E_c - E_0$ rises from 0.3 to 1.2 eV.

CONCLUSIONS

The constant energy positions of the Van Hove singularities in the reflection spectra of amorphous SiO$_2$ and a-quartz, the absence of broadening of the peaks in the reflection spectra[26], and a comparison of the x-ray spectra of amorphous and crystalline SiO$_2$ (Ref. 11) indicate that the main features in the electron spectrum of ionic-covalent solids is governed by the short-range order. The results of the present investigation make it possible to extend this conclusion to the case of solids characterized not only by topological disorder but also by local fluctuations of the atomic composition. The presence of the density-of-states peaks in the spectrum of a-SiN$_x$O$_y$ is due to the existence of Si–N and Si–O bonds.

The structure of amorphous silicon oxynitride is described by the model of a disordered randomly connected network or the random bonding model. An atom of silicon in this network does not have a tetrahedral environment, the atoms in N and O displace one another in a random manner, an atom of N has a trigonal coordination, and an atom of O is bound to two Si atoms.

It should be stressed that near the top of the valence band the electron states in a-SiN$_x$O$_y$ are formed not only by the $2p_\pi$ nonbonding orbitals of N and O, but also by the bonding $3s$ and $3p$ orbitals of Si and the $2p$ orbitals of N and O. In terms of the energy band structure the top of the valence band is degenerate. In the case of the narrow $2p_\pi$ bands of O in SiO$_2$ (Ref. 19) and of N in Si$_3$N$_4$ (Ref. 20) the effective mass of holes is anomalously high: $m_h^*(\text{SiO}_2) \approx 10m_0$ and $m_h^*(\text{Si}_3\text{N}_4) \approx 3m_0$. The bonding orbitals near the top of the valence band of these materials correspond clearly to $m_h^* \approx m_0$. This is of fundamental importance because anomalously high values of m_h^* provide the basis for explaining the anomalously low mobility of holes in SiO$_2$ (Ref. 27), and it is used in Ref. 28 to interpret the transport of holes in a-Si$_3$N$_4$.

More rigorous calculations of the density of states in the conduction bands of Si$_3$N$_4$, Si$_2$N$_2$O, and SiO$_2$ are needed to determine the nature of the low-energy maxima in the $L_{2,3}$ and K absorption spectra of Si corresponding to the band gap.

The much steeper rise of the $L_{2,3}$ absorption edge of Si of the crystalline material, compared with the calculated density of states, has stimulated an experimental study[29] aimed to detect excitons near the $L_{2,3}$ absorption edge of Si using synchrotron radiation. However, the results reported in Ref. 29 could not be used to draw a definite conclusion on the existence of excitons in Si. Theoretical representations in the RB model were developed by investigating the structure of a-SiO$_x$. However, the experiments showed that amor-
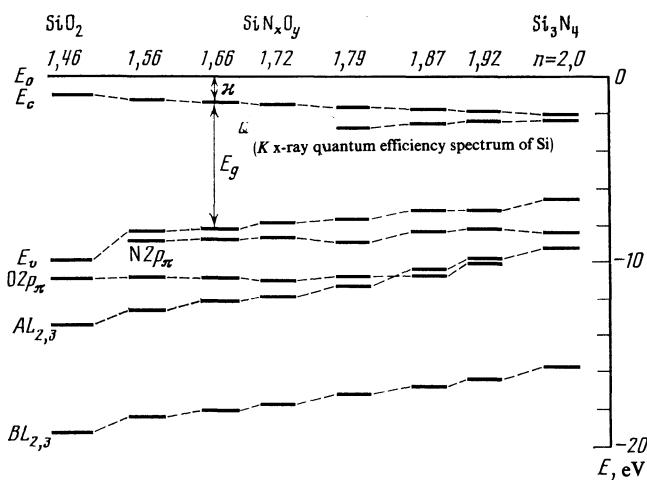

FIG. 8. Energy diagram of the levels (relative to the electron energy in vacuum) obtained for SiO$_2$, SiN$_x$O$_y$, and Si$_3$N$_4$: $\varkappa$ is the electron affinity which sets the position of the bottom of the conduction band E_c; E_g is the width of the band gap.

phous SiO_x films prepared by a method similar to that used to obtain a-SiN_xO_y are described by the RM model, i.e., in the first approximation they represent a mixture of SiO_2 and Si clusters.[6] Dissociation of SiO_x into SiO_2 and Si is clearly due to the fact that in the case of SiO_x the topological conditions for the saturation of bonds and dense packing are not satisfied in SiO_x.

A comparison of the experimental results with the theoretical predictions based on calculations of the electron structure of Si_2N_2O made from first principles[7] indicate that the theoretical results agree qualitatively with the experiments, but several effects not predicted by the theory are observed experimentally. A quantitative agreement between the experiments and calculations in respect of the energy positions of the density-of-states peaks is also quite good.

[1)] Institute of Semiconductor Physics, Siberian Branch of the Academy of Sciences of the USSR, Novosibirsk.

[1] J. M. Ziman, Models of Disorder: Theoretical Physics of Homogeneously Disordered Systems, Cambridge University Press, 1979 (Russ. Tansl., Mir, M., 1982).

[2] M. Misawa, T. Fukunaga, K. Nichara, T. Hirai, and K. Suzuki, J. Non-Cryst. Solids 34, 313 (1979).

[3] I. Idrestedt and C. Brosset, Acta Chem. Scand. 18, 1879 (1964).

[4] W. Y. Ching, Phys. Rev. B 26, 6610 (1982).

[5] R. J. Temkin, J. Non-Cryst. Solids 17, 215 (1975).

[6] V. A. Gritsenko, Yu. P. Kostikov, and I. A. Romanov, Pis'ma Zh. Eksp. Tero. Fiz. 34, 6 (1981) [JETP Lett. 34, 3 (1981)].

[7] W. Y. Ching and Shang-Yuan Ren, Phys. Rev. B 24, 5788 (1981).

[8] V. A. Gritsenko, N. D. Dikovskaya (Dikovskaja), and K. P. Mogilnikov, Thin Solid Films 51, 353 (1978).

[9] S. I. Raider, R. Flitsch, J. A. Aboaf, and W. A. Pliskin, J. Electrochem. Soc. 123, 560 (1976).

[10] I. A. Brytov and Yu. N. Romaschenko, Fiz. Tverd. Tela (Leningrad) 20, 664 (1978) [Sov. Phys. Solid State 20, 384 (1978)].

[11] I. A. Brytov, V. A. Gritsenko, Yu. P. Kostikov, E. A. Obolenskiĭ, and Yu. N. Romashchenko, Fiz. Tverd. Tela (Leningrad) 26, 1685 (1984) [Sov. Phys. Solid State 26, 1022 (1984)].

[12] V. A. Gritsenko, Yu. P. Kostikov, and S. P. Sinitsa, Izv. Akad. Nauk SSSR Neorg. Mater. 19, 408 (1983).

[13] M. J. Rand and J. F. Roberts, J. Electrochem. Soc. 120, 446 (1973).

[14] T. P. Smirnova, S. M. Repinskiĭ, and F. L. Édel'man, V kn.: Nitrid kremniya v élektronike (in: Silicon Nitride in Electronics), Novosibirsk, Nauka, 1982.

[15] G. W. Wertheim, in: Electron and Ion Spectroscopy of Solids (ed. by L. Fiermans, J. Vennik, and W. Dekeyser) (Russ. Transl.), Mir, M., 1981.

[16] A. P. Lukirskiĭ and I. A. Brytov, Fiz. Tverd. Tela (Leningrad) 6, 43 (1964) [Sov. Phys. Solid State 6, 32 (1964)].

[17] É. Z. Kurmaev, V. G. Zyryanov, I. Ya. Guzman, and T. N. Zabruskova, Izv. Akad. Nauk SSSR Neorg. Mater. 9, 867 (1973).

[18] J. Robertson, Philos. Mag. B 44, 215 (1981).

[19] Shang-Yuan Ren and W. Y. Ching, Phys. Rev. B 23, 5454 (1981).

[20] J. R. Chelikowsky and M. Schluter, Phys. Rev. B 15, 4020 (1977).

[21] E. Martinez and F. Yndurain, Phys. Rev. B 24, 5718 (1981).

[22] W. Y. Ching, Phys. Rev. B 26, 6633 (1982).

[23] R. Hezel and N. Lieske, J. Appl. Phys. 51, 2566 (1980).

[24] H. M. Lenning, I. O. Edwards, and M. Richman, Inorg. Chem. Acta 20, 1 (1976).

[25] A. G. Revesz, Phys. Status Solidi A 57, 235 (1980).

[26] H. R. Philipp, J. Phys. Chem. Solids 32, 1935 (1971).

[27] T. H. DiStefano and D. E. Eastman, Phys. Rev. Lett. 27, 1560 (1971).

[28] Z. A. Weinberg and R. A. Pollak, Appl. Phys. Lett. 27, 254 (1975).

[29] F. C. Brown, R. Z. Bachrach, and M. Skibowski, Phys. Rev. B 15, 4781 (1977).

Translated by A. Tybulewicz